Major Components which affecting on the performance of tadpole structured electric vehicle are Chassis/Frame, Upright with A- Arms and rear swing arm. Design and optimization of this component is essential to optimize the performance of vehicle based on weight criteria.

4.1 Chassis/ Frame Design

4.1.1 Design Considerations

The chassis design, which was among the most critical elements to be completed, was tasked with integrating every vehicle component into a singular, functional vehicle. The procedure by which the chassis was designed was as follows:

- Weldable sections were incorporated into the chassis to facilitate the attachment of components using fasteners.
- Analysis was conducted to verify the structural integrity of the chassis. FEM analysis was performed on the chassis to determine its frequency and strength response. Members were added or member thickness was adjusted until the chassis achieved adequate strength.
- The chassis underwent manufacturing preparations. Individual tube components were identified and their profiles were specified in a manner that facilitated assembly and manufacturing.
- Placing the obtained suspension points on the chassis.
- Designing the driver compartment for the suitable driver and to satisfy the ergonomics requirements.
- Assuring the proper node-to-node triangulation.

4.1.2 Material Selection

The material selected for the chassis is AISI 4130 steel. It is a versatile alloy steel with very good strength, fatigue strength and weldability. For properties material is tested in the laboratory OM Meta Lab Services PVT. LTD.

Table 4.1: Material Properties of AISI 4130

Property	Observed Value
OD (mm)	25.40
ID (mm)	23.42
% Elongation	19.12

Property	Observed Value
Thickness (mm)	1.01
Density (Kg/m^3)	7850
Poisson Ratio	0.29
Modulus of Elasticity (Gpa)	205
Tensile Strength (N/mm^2)	679.67
Yield Strength (N/mm^2)	594.31

In the construction of this automobile, a decision was made to utilize 25.4 mm tubing in various thicknesses between 1 mm and 1.2 mm for the tube members. Where necessary, sheet steel was incorporated into the design. The 25.4 mm tube diameter provided an extensive selection of tube thickness options and satisfied the chassis's strength requirements. Maintains a low-to-the-ground profile and a straightforward design, but fails to adequately safeguard its occupants in the event of a rollover, an occurrence that is more frequent in urban vehicles compared to conventional cars. As a consequence, a roll cage was incorporated into the design of the chassis. However, in order to facilitate the incorporation of future structural body designs onto the vehicle, the roll hoop was intentionally engineered to be detachable. In order to accomplish the goal of a removable roll hoop, two distinct chassis components—the primary body and the roll hoop—were fabricated and could be bolted together as needed. With the completion of the primary chassis components, the sheet metal mounting tabs were affixed to the chassis components. Every tab was specifically engineered to be produced using a waterjet or laser cutting technique, followed by jigging into the chassis for welding. With the exception of the 3 mm and finer tabs, which were intended to be bent, all other sizes were constructed to be welded to the chassis. This method permits the fabrication of tabs with small tolerances at the frame and mount locations through the incorporation of tab-specific alignment features, such as a profile of the tube member. With the aid of these characteristics, the tabs on the chassis could be readily located.

4.1.3 Wheelbase and track

It is challenging to precisely determine the optimal wheelbase, which is the distance between the centerlines of the axles on a vehicle. On winding circuits, short-wheelbase vehicles are typically more agile and adept at tight turns, whereas long-

wheelbase vehicles maintain greater stability on rapid straightaways. Hillclimb and sprint cars, which are typically required to traverse narrower roads with tighter hairpins, have developed wheelbases ranging from 2000 to 2500 mm. It is simpler to specify the optimum track, which is the distance between the centers of the axles of a vehicle. It can be seen that weight transfer decreases as track T increases. Moreover, a broad track decreases cornering roll. Frequently, the regulations are expressed in terms of the vehicle's utmost overall width, which results in the wider rear wheels having a slightly narrower track than the front wheels. The tight and winding circuits require a vehicle that is both lightweight and exceptionally agile. Studies have shown that compact automobiles with a track of 1200 mm and a wheelbase between 1500 and 1700 mm perform the best. Considering all parameters like city road conditions wheelbase and track have been optimized as 1800 mm and 1200 mm respectively keeping 60 % ratio for optimum performance of the vehicle.

4.1.4 Position of centre of mass of a vehicle

During the preliminary design phase, it is essential to make an estimate of the center of mass for each primary component as it is integrated into the system. Subsequent modifications may be implemented to the ultimate positional correlation between the constituent elements and the wheels, with the aim of achieving the desired allocation of weight between the front and back. In order to graphically represent the process, Figure 1.4 showcases a restricted set of components together with the distances between their separate centers of mass and a shared point. In this case, the front contact patch, represented as x, is the shared element.[53]

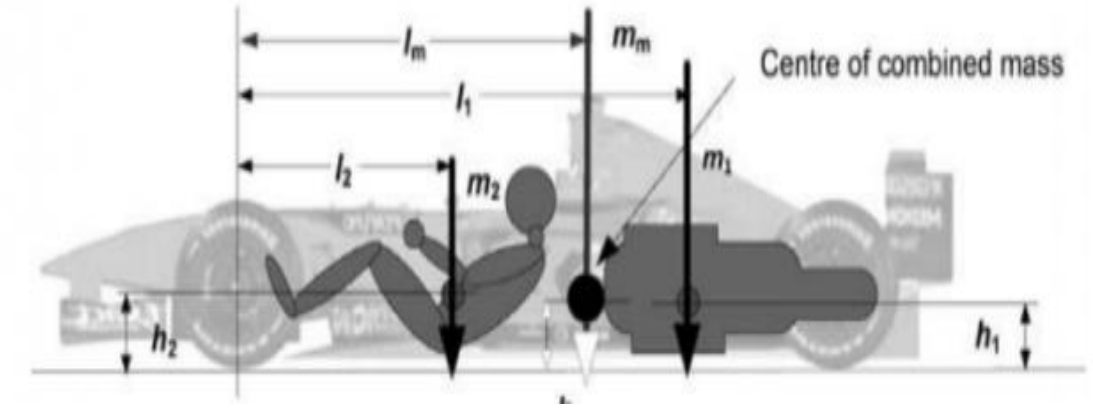

Figure 21 : Position of the Center of mass [53]

Either an estimation or measurement is performed on the magnitude (m) and location (l, h) of the center of mass of each individual component. Determining the location of the combined mass (mm) in relation to the common point (lm) and hm is the objective.

Simply summing the masses of the constituent components yields the total mass. For a set of n number components in total, this is mathematically represented as:

$$m_m = \sum(m_1 + m_2 + \cdots \ldots \ldots m_n) \quad \text{(4.1)}$$

The location of the combined center of mass is:

$$l_m = \frac{\sum(l_1 m_1 + l_2 m_2 + \cdots l_n m_n)}{m_m} \quad \text{(4.2)}$$

$$h_m = \frac{\sum(h_1 m_1 + h_2 m_2 + \cdots h_n m_n)}{m_m} \quad \text{(4.3)}$$

By ensuring that the combined mass of the components exerts the same moment about the front contact patch as the sum of the masses of the individual components, the procedure described above is straightforward.

Table 4.2: Center of Mass of Vehicle

Component	Mass		Horizontal Distance from front axle	Horizontal moment	Vertical distance from ground	Vertical moment
	(kg)		(mm)	(kg-mm)	(mm)	(kg-mm)
Car						
Front-wheel assembly	21		0	0	200	4200
Pedal box	2		0	0	200	400
Steering gear	5.5		100	550	300	1650
Controls	3		300	900	800	2400
Frame + floor	23		800	18400	700	16100
Body Works	30		800	24000	700	21000
Fire extinguisher	3		1000	3000	600	1800
Motor	9		1780	16020	200	1800
Battery Pack	30		1200	36000	700	21000
Battery 12 V	2		1200	2400	700	1400
Controller &	10		1200	12000	700	7000

Component	Mass		Horizontal Distance from front axle	Horizontal moment	Vertical distance from ground	Vertical moment
	(kg)		(mm)	(kg-mm)	(mm)	(kg-mm)
Ele. Panel						
Rear Swing	5		1780	8900	200	1000
Electrical	7		1200	8400	700	4900
Mescellinoius				0		0
Total car	**150.5**		**812**	**122170**	**530**	**79750**
Driver						
Drivers Weight	80	Distance between front axle to pedal face	700			
Feet	2.8	40	740	2052	250	693.3333
Calves	7.7	200	900	6912	430	3302.4
Thighs	17.3	560	1260	21773	600	10368
Torso	36.9	800	1500	55360	650	23989.33
Forearms	3.2	530	1230	3936	700	2240
Upper arms	5.3	800	1500	8000	840	4480
Hands	1.3	330	1030	1318	820	1049.6
Head	5.5	830	1530	8486	1110	6156.8
Total driver	**80**	**4090**	**9690**	**107837.87**	**653**	**52279.47**
Grand total	230.5		**998**	230008	**573**	132029.5
Rear load	129					
Front load				101		
Ratio F/R			**43.9%**	**56.1%**		

4.1.5 Individual Static Wheel Loads and Front to Rear Weight Balance

The static case pertains to the loads experienced by the vehicle in the absence of accelerations caused by deceleration, cornering, or acceleration. The vehicle ought to be evaluated while it is completely loaded with the driver. The following burdens would be assessed in the pits if the vehicle were to be positioned on a level surface. Thus far, the bulk of components has been denoted in kilograms. The terms 'load' and 'weight', nevertheless, refer to force, which is naturally expressed in Newtons. We will therefore henceforth consider the forces, denoted as W, acting on the vehicle.[87]

Where, Force (N) = mass (kg) x acceleration (m/s^2).

where, for vertical loads, the acceleration = g = 9.81 m/s^2.

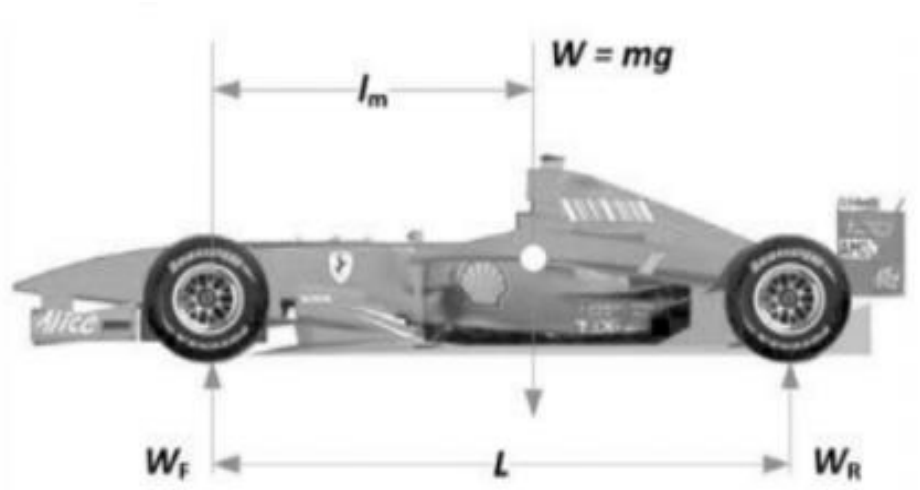

Figure 22 : Static Wheel Loads

To ascertain the load on the rear axle, WR, we need only measure the moments about the front axle and the horizontal position of the center of mass.

Weight distribution on the rear axle,

$$W_R = W\ X\ \frac{l_m}{L} \quad \text{..... 4.4}$$

From vertical equilibrium:

Weight distribution on the front axle,

$$W_F = W - W_R \quad \text{..... 4.5}$$

Figure 22. represents a free-body diagram. In order for the car to remain in a state of static equilibrium while floating weightlessly in space, the three forces at play, W, WF, and WR, must balance each other. Specifically, the downward force of gravity, W, must be equal and opposite to the combined forces exerted by the wheels, WR and WF. The upward display of wheel forces is attributed to this reason. They denote the exertion of the road's forces on the car.

The designer has the ability to manipulate the distribution of weight between the front and rear of the vehicle by strategically relocating specific components, such as the battery or electronic elements. Modifying the location of the front and/or rear axles in relation to the battery and motor's major mass leads to a notable difference. What is

the ideal ratio of weight distribution between the front and back of a vehicle? From a practical perspective, it might be contended that a 50:50 ratio is the most favorable. Nevertheless, as we will soon observe, having a greater amount of weight over the wheels that provide propulsion offers a distinct benefit when it comes to accelerating from a stationary position. Cars often strive for a front/rear ratio of approximately 45:55 and tackle the handling problem by utilizing bigger rear tires.[47]

4.1.6 Un-sprung mass lateral force

Lateral load transfer calculations are often performed in lateral g increments. At a lateral acceleration of 1.5 g, the masses of all the vehicles (in kg) are multiplied by the lateral acceleration, Ay, of 1.5 x 9.81 to get lateral forces (N). Normal lateral acceleration for cars is between 0.7 to 0.9. If this value goes above 1.0 it will be good design. So, for our design considering it as 1.25 and calculating lateral forces. Table below shows the individual wheel loads and lateral forces on each wheel.[88]

Table 4.3: Individual Wheel Loads

Lateral g, A_y	**1.25**	
Data	Front	Rear
Wheel radius, r (mm)	200	200
Wheel track, T (mm)	1200	700
Height roll centre, h_{rc} (mm)	200	200
Ride rate, K_R (N/mm)	30	30
Unsprung Mass, M_u (kg)	20	12
Wheelbase, L (mm)	1800	
Sprung mass, M_S (kg)	230	
Height sprung mass, h_{ms} (mm)	200	
Dist, front axle to M_S, l_{ms}(mm)	800	
Wheel loads		
Static loads, R (N)	724.9	560.3
From unsprung mass (N)	40.9	42.0
From sprung mass thro. Links (N)	261.1	358.1
Roll rates (Nm/deg)	377.0	128.3
Roll distribution %	74.6	25.4
From sprung mass thro. springs (N)	0.0	0.0
Total load transfer	302.0	400.2
Inner wheel loads	422.8	160.1
Outer wheel loads	1026.9	960.4

4.1.7 Dimension Parameters & CAD Model

By using solid works and designed parameters chassis generated as CAD model. After several iteration chassis shown in the fig. is selected and further analysed.

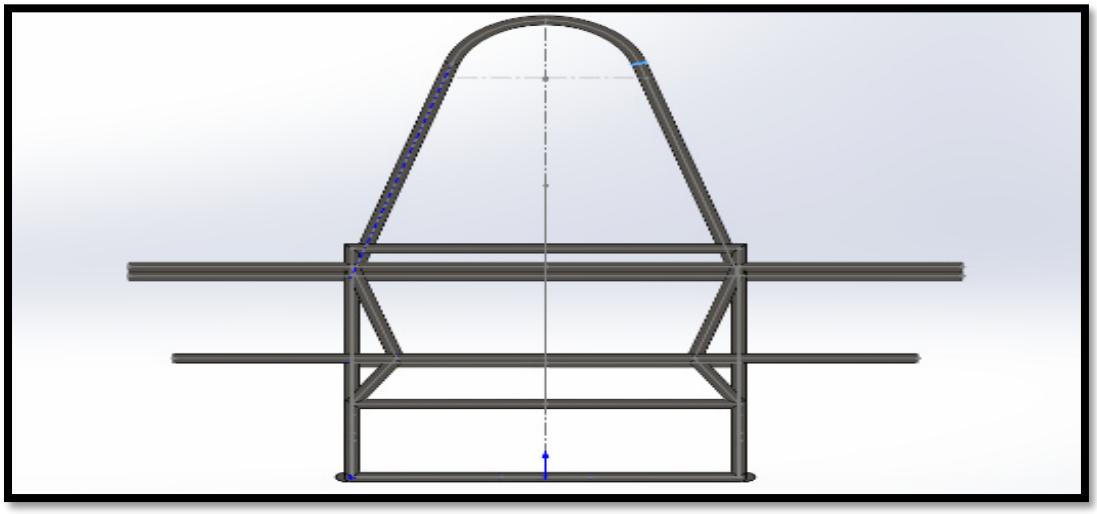

(a)

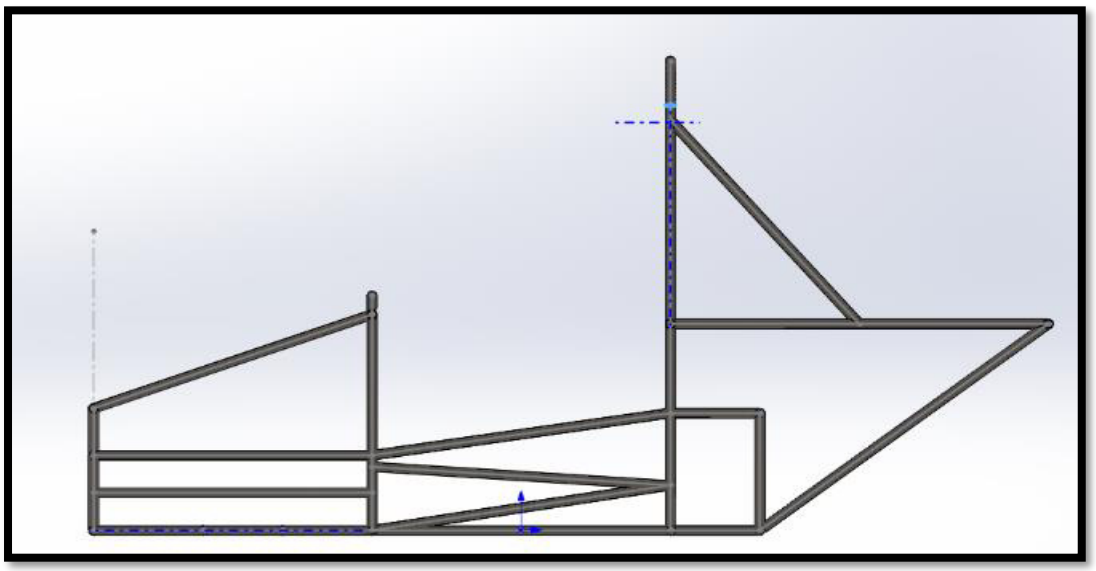

(b)

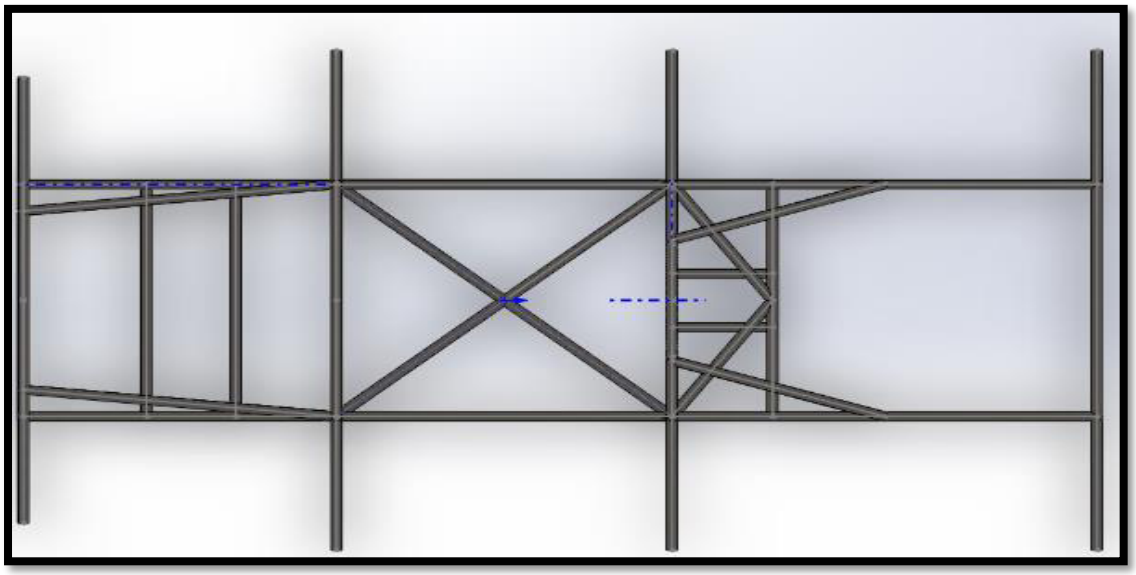

(C)

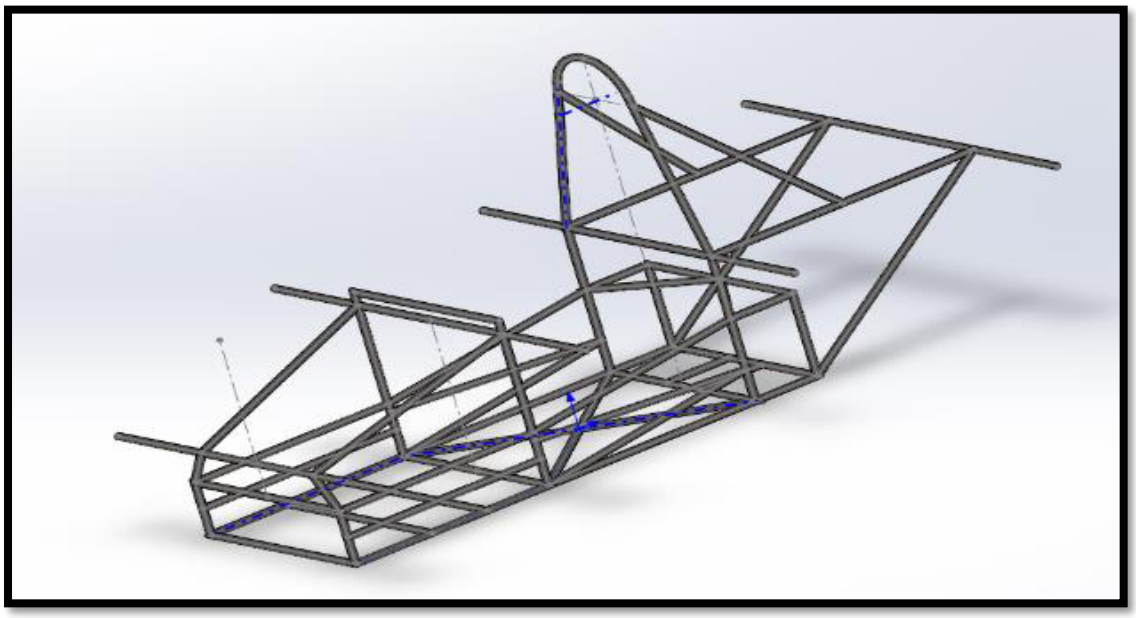

(D)

Fig. 23 : a) Side view of chassis b) Front view of chassis c) Top view of chassis d) Isometric view of chassis

From the CAD model below are the observed parameters of the vehicle chassis and design considerations.

Table 4.4: Estimated vehicle chassis parameters

Description	Value	Units
Total Mass (Approx.)	180	Kg
Mass of Chassis	23	Kg
CG Height	417	mm
Front Wheel To CG Distance	743	mm
Rear Wheel To CG Distance	1057	mm
Wheelbase	1800	mm
Cornering Stiffness, Front Wheel	2500	N/mm
Cornering Stiffness, Rear Wheel	4000	N/mm
Nominal Track Width	1200	mm
Ground Clearance	160	mm

In the structural investigation, boundary conditions and equivalent loads were applied to the chassis, when necessary. Accelerations have more significance compared to the specified quantity of forces for the chassis, therefore being classified as overarching design requirements. The application of forces may be effectively determined by applying a load that is 20 times the acceleration due to gravity in the desired direction. If certain conditions are not met, such as the lack of a tube structure between the driver and a component, it is recommended to utilize a 40g load. Only 20-gram loads were used in this experiment for two particular reasons. The first rationale is derived from the overarching recommendation presented in reference [47], whilst the subsequent rationale is that the suggested acceleration attains a magnitude that has the potential to induce harm, a threshold that has been determined to be appropriate for the chassis to endure, as described in reference [47]. The research assumed that the weight of both the driver and passenger was equivalent to the requirement set by the Fédération Internationale de l'Automobile (FIA). This regulation specifies that the harness we have selected is intended to accommodate a weight of 80 kg. The evaluation will consider the tube members as beam elements, whilst the sheet metal linked with them will be analyzed as solid elements. The use of this simplified analytic approach is well-suited for tube member chassis, resulting in a significant reduction in the computing complexity of the research [4]. In order to improve the accuracy of the model, mesh refinement was conducted on components that exhibited

significant strain rates. It was essential to enhance the element density of the tube members connected to solid elements, since the transmission of forces was limited to the nodes. All connections that were welded were categorized as bonded. The bolt of the roll hoop was designed to establish a connection by applying a preload of 25 Nm and implementing a lock mechanism that effectively prevents any ingress between the surfaces being attached. The primary determinant influencing the time of the model's execution was the absence of penetration, necessitating around 20 minutes to accomplish for every permutation of boundary conditions. The research may use specific material characteristics, since the producer of the tubes performed several tests on the tubes utilized in the construction of the chassis. Similar to previous finite element analysis, the findings presented in this study provide an estimation of the potential outcomes in real-world scenarios.

4.1.8 Calculations for Load

As per south Asia guidelines for small electric vehicles, the speed is limited by the weight of the car and driver. So while designing the car considering the weight of car is to be 200 kg and the weight of the driver to be 80 kg. Hence by using the formula for maximum force (F_{max}) applied on the car with driver.[53]

$$F_{max} = \text{mass} \times \frac{\text{velocity}}{\text{time}} \quad \text{..... (4.6)}$$

where time (t) is the time of contact between the car and impact load which is 0.5 s, Velocity is 15 m/s (Approx. 55 KMPH) and mass is 280kg. (considering maximum)
Therefore,

$$F_{max} = 280 \times \frac{15}{0.5} = 8400\ N$$

For being safe side considering,

$$F_{max} = 10000\ N$$

This is the force used for front, rear and side impact analysis of chassis.

4.1.9 Impact Analysis

1. Front Impact Analysis

An off-axis frontal impact occurs when a vehicle collides with a huge object, such as a wall or building, while traveling at a high speed. The event is represented as a 20g

acceleration, accompanied by a minor off-axis force component. The following boundary conditions were applied for a total vehicle mass of 280 kg:

Forces – $F_X = -10\ KN$, $F_y = 0\ KN$, $F_Z = 0\ KN$

Located in the foremost part of the vehicle's structure, these tube members are the first to come into contact after an impact, excluding the bumper members that protect the wheels.

Fixtures – The primary roll hoop's bottom nodes allow for unfettered rotation while maintaining a fixed displacement.

Acceptance Criteria – Absence of stress failures that pose a risk. Figure a) displays the stresses of the beam members, Figure b) illustrates the strain, and Figure c) presents the deflection.

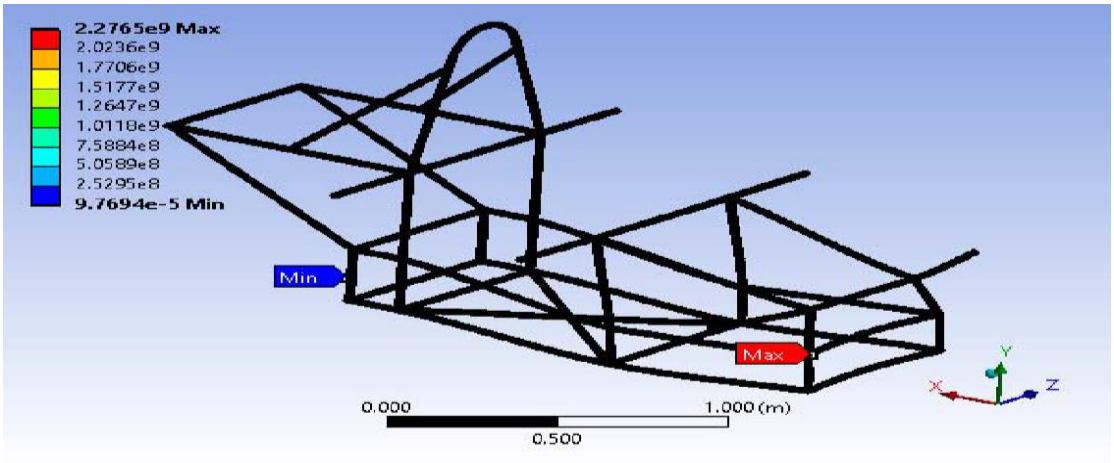

a)

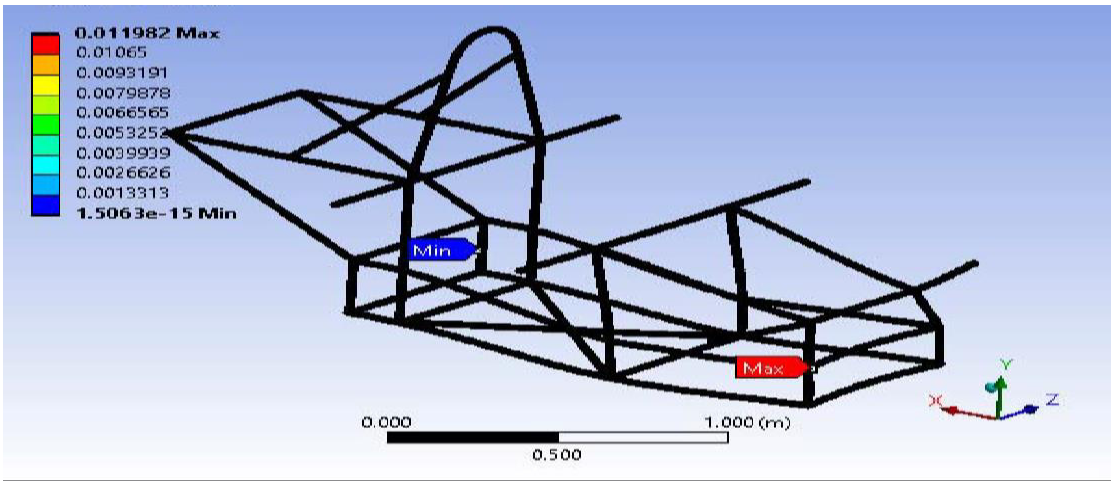

b)

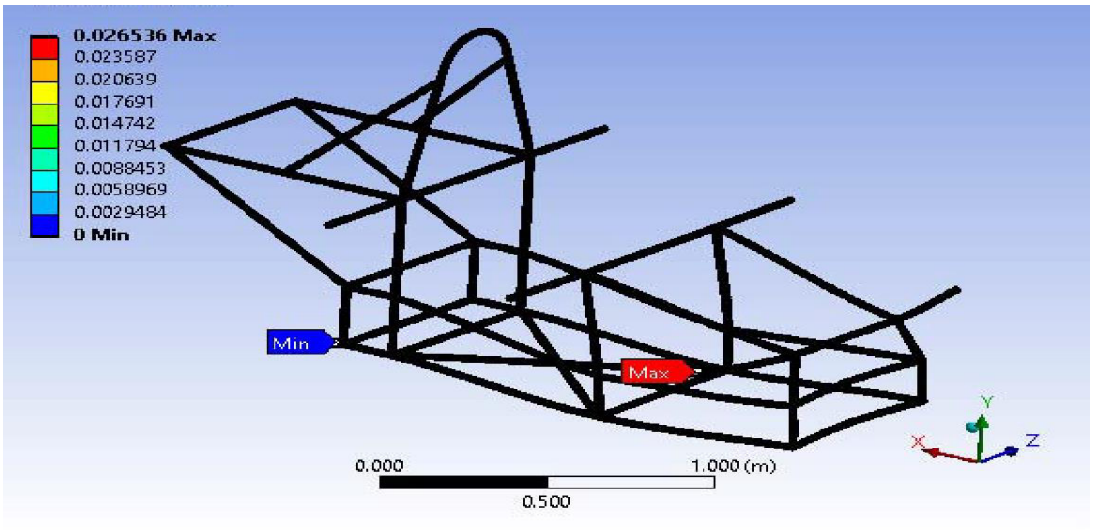

c)

Fig. 24 : a), b) and c) Showing Front Impact Analysis

The stress plot clearly shows that the frame fails in two elements of the bumper members when subjected to loading, while the remaining chassis members remain below the yield stress of the material. The failure of the bumper material is not a cause for concern, as its primary function is to prevent pedestrians from entering the wheel wells, rather than providing structural reinforcement. The chassis components that secure the driver are well below the yield stress and will provide enough protection for them. If the front members fail, it is likely that the other members will experience greater deformation and stress. Nevertheless, due to the minimal stress levels, the members should have the capacity to withstand the additional strain. The deformation plot exhibits conventional deflection patterns, characterized by a relatively low magnitude. The chassis exhibits a propensity to deform upwards in the absence of any vertical force. The probable cause for this is the heightened stiffness in the lower layer of the chassis compared to the upper layer, as evidenced by the implementation of diagonal cross members.

Table 4.5 : Front Impact Analysis Results

Parameters	Maximum Values
Stress	2.276 X 10^9 N/m^2
Strain	11.982
Deflection	26.53 mm
Factor of Safety (F.O.S.)	**8.3**

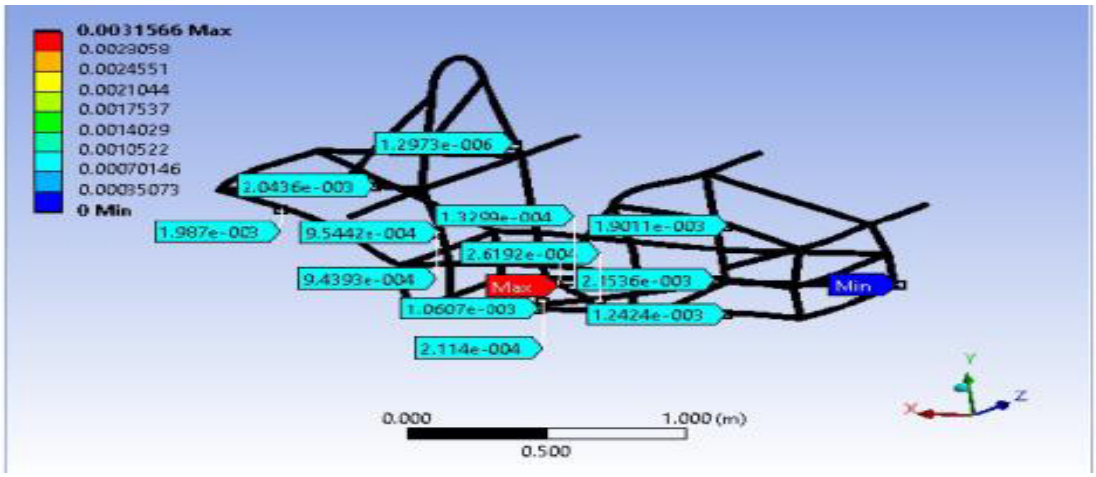

d)

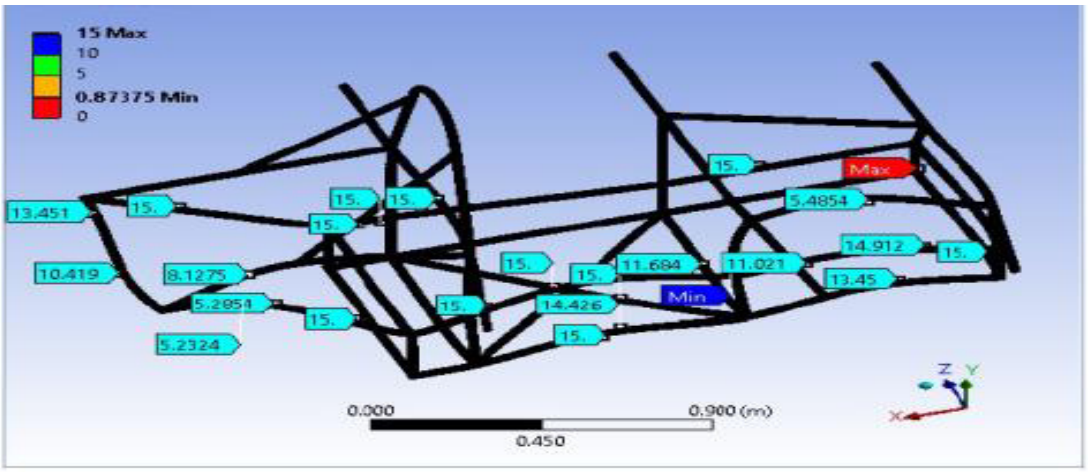

e)

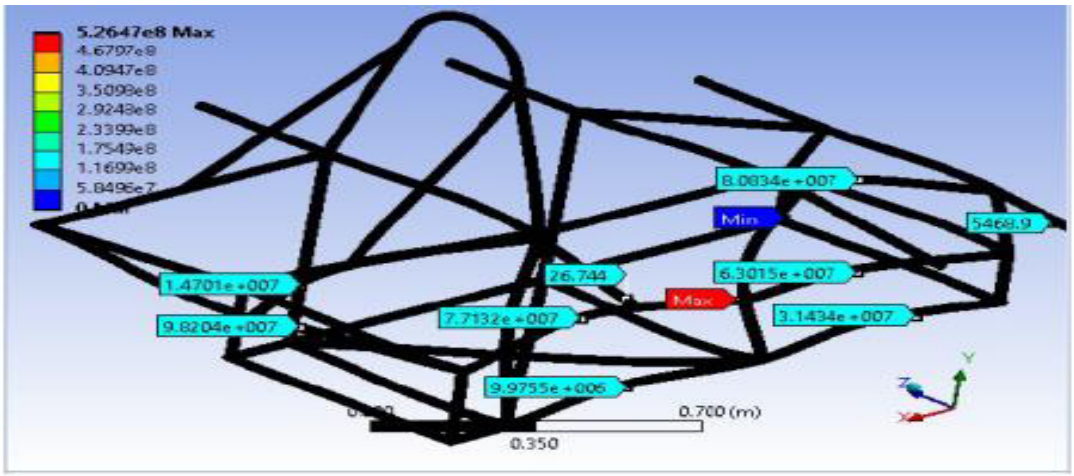

f)

Fig. 25 : d), e) and f) Showing Side Impact Analysis

Table 4.6 : Side Impact Analysis Results

Parameters	Maximum Values
Stress	5.26 X 10^8 N/m^2
Strain	2.86
Deflection	3.156 mm
Factor of Safety (F.O.S.)	**9.67**

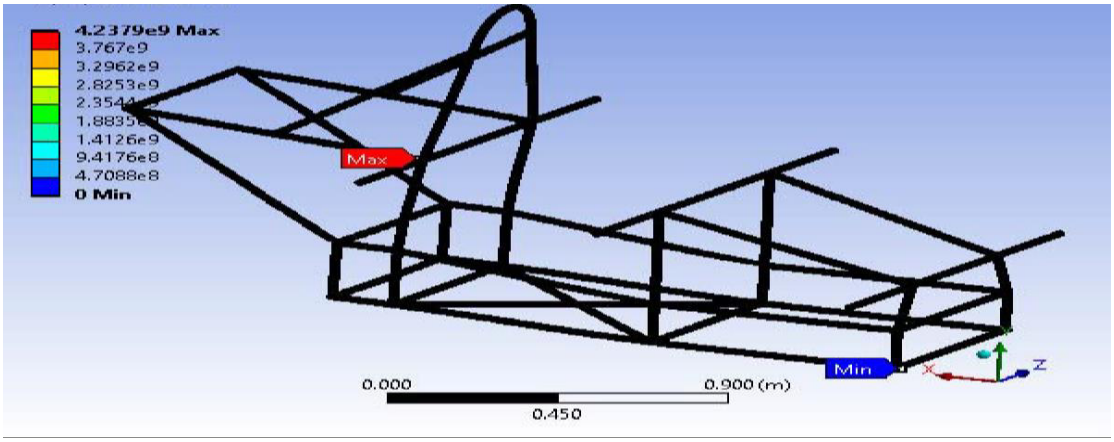

(g)

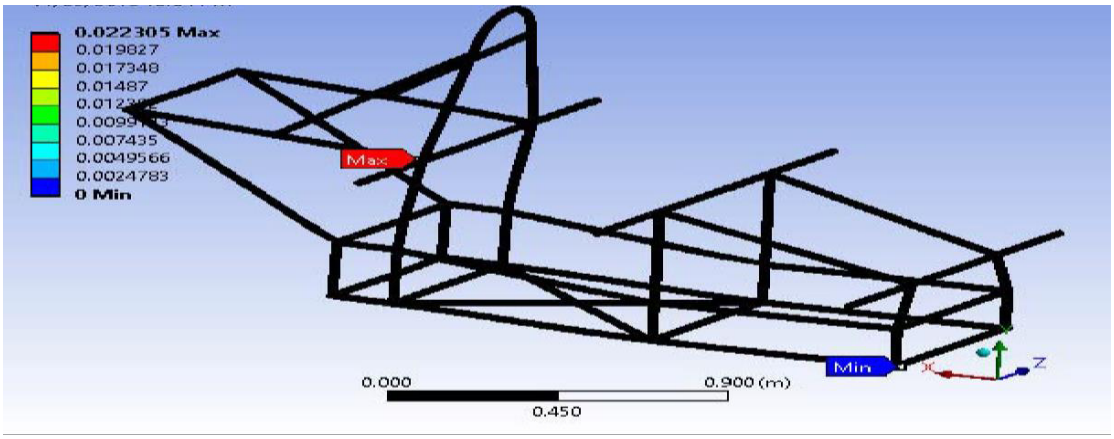

(h)

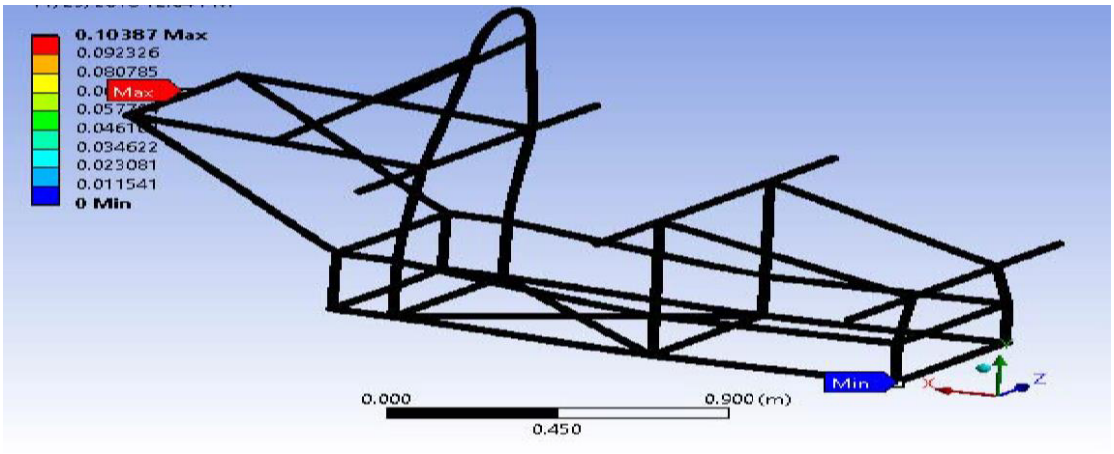

(i)

Fig. 26 : g), h) and i) Showing Rear Impact Analysis

Table 4.7 : Rear Impact Analysis Results

Parameters	Maximum Values
Stress	4.24 X 10^9 N/m^2
Strain	22.3
Deflection	103.87 mm
Factor of Safety (F.O.S.)	**6.13**

(Note: Pipes on which Upper spring points are mounted are of 1inch x 1.6mm while all other pipes are of thickness 1inch x 1mm for strength enhancement purpose.)

Table 4.8 : Iteration of Chassis

Parameter	Iteration-I	Iteration-II	Iteration-III	Iteration-IV	Iteration-V
FOS (Min.)	10.23	8.3	7.9	6.9	6.13
Weight (Kg)	30.2	27.9	24.8	23	20

Fifth iteration from the results gives better strength as FOS is more than 6 and weight of the chassis reduced by 10.2 Kg. So, for further consideration iteration five will be selected in the design.

4.2 Rear Wheel Assembly Design

4.2.1 Selection of Motor

As per the guidelines of south Asia small EV manufacturing for intermediate speed vehicle selecting motor of 1500 Watt. On the basis of weight, selected the motor with

minimal power consumption, to contribute in weight reduction of vehicle. As the power consumption of motor increases price also increases. So, opted minimum range of motor to keep our vehicle under minimum budget. Allowable power for the motor up to 5000 Watt. So, to have our peak current minimum, we opted for optimized motor i.e., of 1500 Watt. [66]

Table 4.9 : Peak Current Calculation

Parameter	Case -I	Case -II
Peak Power (Watt)	1500	2000
Voltage (V)	48	48
Peak Current (A) (I= $\frac{P}{V}$)	31.2	41.6

Hence, based on our prototype requirement, selected 1500-Watt motor. As minimum and if selecting for higher range of motor, current requirement will also increase leading to sudden load on battery. Because of which the battery will drain faster than the required consumption.

Table 4.10 : Specifications of selected motor

Specification	Value
Rated Voltage	48 Volt
Rated Power	1500 Watt
Rated Speed	600 – 900 RPM
Rated Torque	15 – 45 N-m
Maximum Speed	45- 60 KMPH
Weight	9 Kg
Rated Current	20 – 40 A
Continuous Discharge Current	10 -15 A
Load Consideration	250– 900 Kg

A. Design Consideration:

It depends upon the weight constraints of the vehicle that is 280 Kg with drive. Also, the torque is 10 N-m for 280 Kg.

B. Torque Calculation Given:

Power (P) = 1.5 KW

Rim dia. = 14 inch = 355.6 mm

R = 0.178 m = 178 mm

μ = 0.017 = 0.02

Tractive Force:

$$F_t = \mu mg \quad \text{..... (4.7)}$$

Starting Torque:

$$T = F_t \, X \, R \quad \text{..... (4.8)}$$

$$a_{max} = \frac{(Total\ Max\ Torque - Required\ Torque)}{m \, X \, R} \quad \text{..... (4.9)}$$

where,

μ = coefficient of friction

g = gravitational force

m = mass

R = radius of wheel

a_{max} = maximum acceleration

Table 4.11 : Calculation of Maximum Acceleration

Parameter	Case I (m= 280 Kg)	Case II (for m=260 kg)	Case III (for m=240 kg)
$\mathbf{F_t}$	54.936	51.02 *N*	47.088 *N*
T	9.778 N-m	9.081 N-m	8.381 N-m
$\boldsymbol{T_{max}}$	45 N-m	45 N-m	45 N-m
$\boldsymbol{a_{max}}$	0.706 m/s^2	0.776 m/s^2	*0.857* m/s^2

4.2.2 Swing Arm

A. Material Selection

Lightweight structural materials allow automobiles to carry improved emission control, safety, and integrated electrical systems without adding weight. Hybrid, plug-in, and electric cars need lightweight materials. Lightweight materials may reduce the weight of power systems like batteries and electric motors, enhancing efficiency and all-electric range. Lightweight materials might reduce battery size and cost while maintaining plug-in car all-electric range. [90]

Lightweight materials' cost, recycling, integration with cars, and fuel efficiency advantages depend on research and development. The most commonly used materials for lightweight structures in automotive industries and their properties of it are given below.

Table 4.12: Material Properties

Material	Tensile Strength (MPa)	Approximate Cost Per Kg. (Rs.)
High strength steel	500	125
Advanced high-strength steel	700	175
Glass fiber composites	3500	200
Titanium	1400	5500
Aluminum and Al matrix composites	240	200
Carbon fiber composites	3500	8000
Magnesium	440	90
7076 T6 Aluminium Alloy	570	600

It is crucial to consider the particular needs and restrictions of the system being optimized while thinking about design factors. This comprises elements including price, size, and performance objectives. By considering the cost-effectiveness and strength of the material used for the automobile and ease in manufacturing 7076 T6 Aluminium alloy material is selected for the swing-arm of a tadpole structured electric vehicle.

B. Generative Design Approach

By using Solid works software CAD model of the swing arm is prepared and assigned given properties to the model.

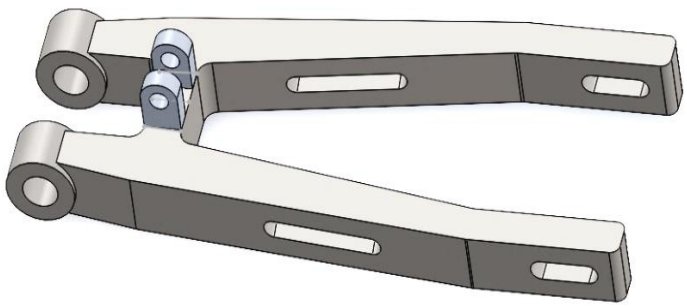

a) Iteration 1

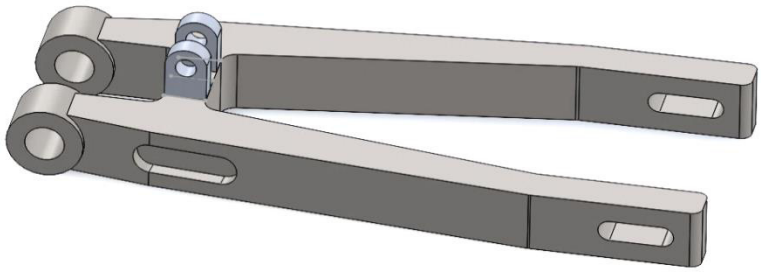

b) Iteration 2

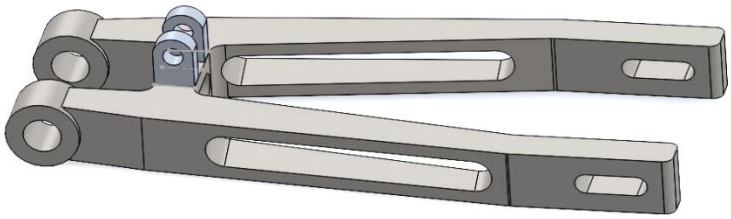

c) Iteration 3

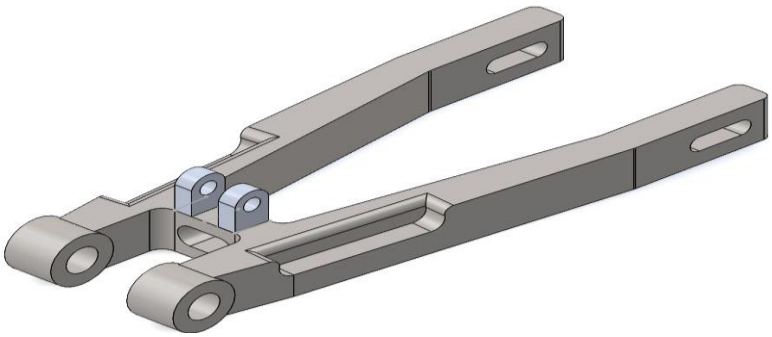

d) Iteration 4

Fig. 27 : Weight and Shape Optimization Iterations

The initial Weight of the Swing Arm was 11.70 Kg. After application of the generative design concept and getting different iterations as follows with varying mass.

Table 4.13: Weight Reduction and it's percentage

Iterations No.	Mass (Kg)	Mass Reduction %
Iteration 1	11.08	2.3%
Iteration 2	11.41	1.00%
Iteration 3	8.75	25.22%
Iteration 4	10.80	7.7%

C. Load Applied for Analysis

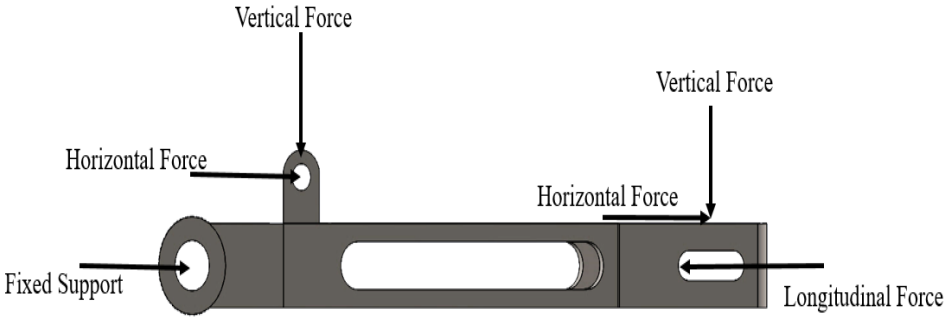

Fig. 28 : Loading Conditions for Rear Swing Arm

In Ansys software loads are applied as shown in Fig. 4. For analysis purpose at the eye end fixed support is considered and vertical forces of 325 N and horizontal force of 1925 N is applied on the swing arm by considering bump due to tire and forces due to suspension. Also, longitudinal force due to acceleration and braking is applied 2000 N.

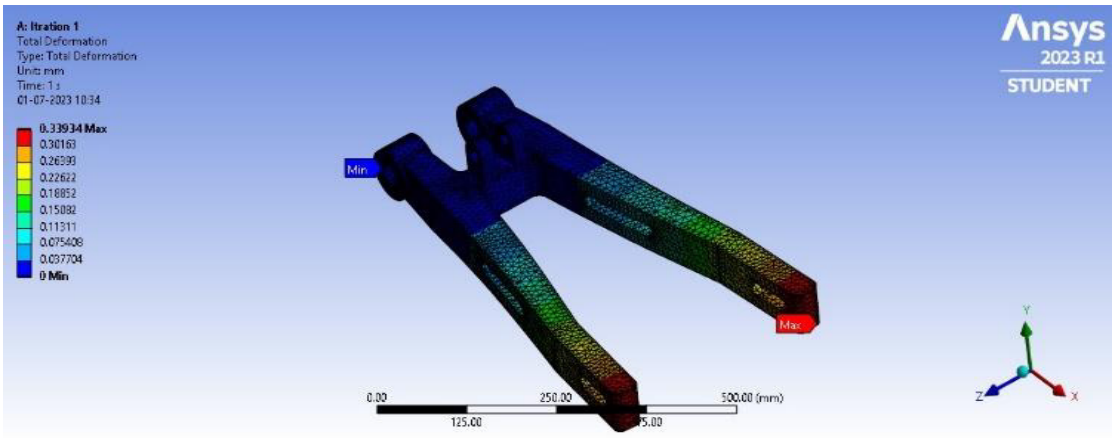

a) Iteration 1

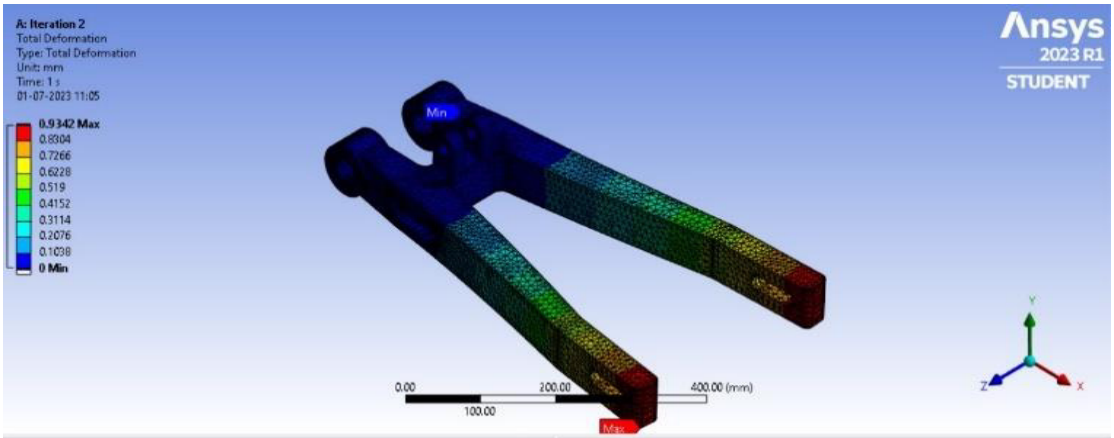

b) Iteration 2

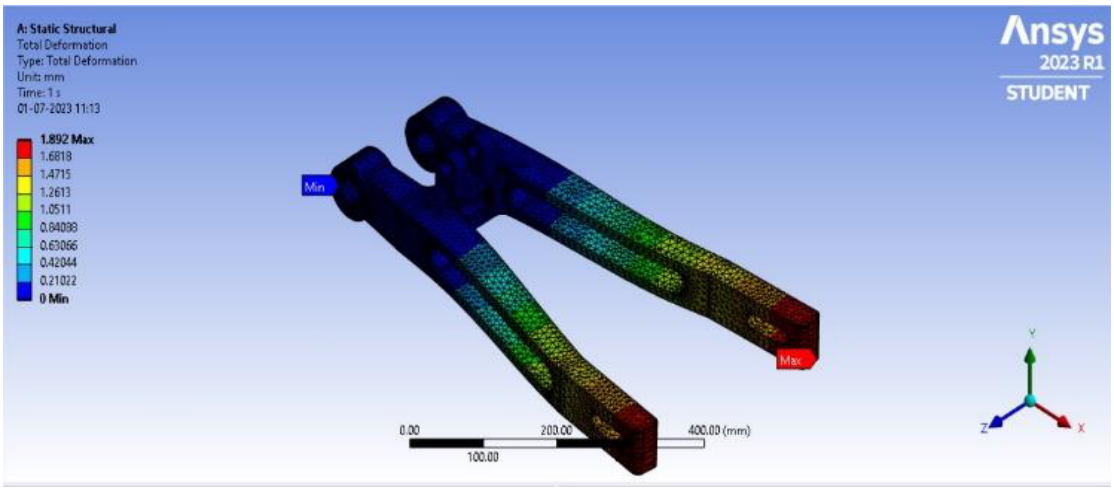

c) Iteration 3

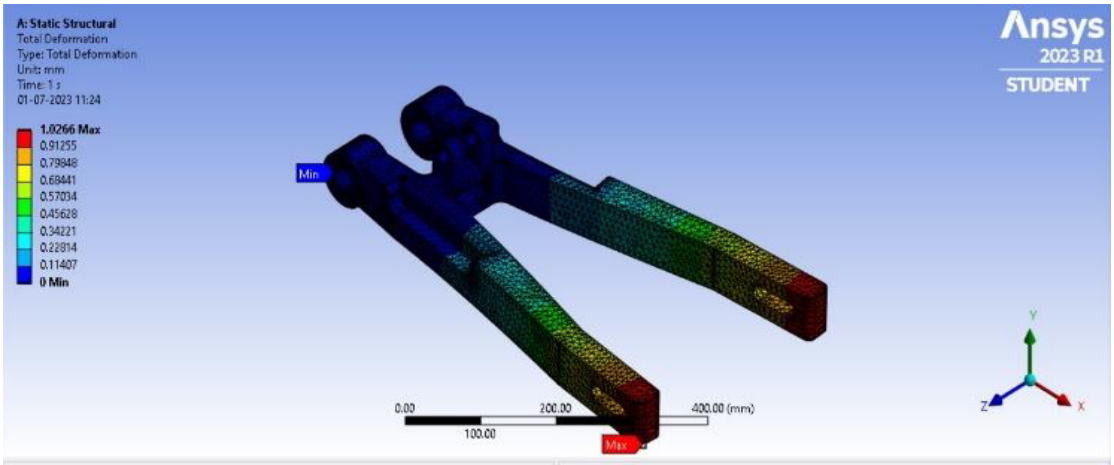

d) Iteration 4

Fig. 29 : Iterations of Rear Swing Arm Analysis by using Ansys Software

Here we are assigning the ranking for the geometry parameters as follows as per the manufacturability and aesthetics of swing arm.

Table 4.14 : Ranking for geometry parameter

Description	Ranking
Low	1
Below Average	2
Average	3
Good	4
Excellent	5

Dividing parameters into beneficial and non-beneficial categories as per their effect on the swing arm as maximum or minimum. So considering Geometry and stiffness as beneficial parameters as they should be maximum and mass, stresses induced, and deformation as non-beneficial parameters as they should be minimum. Values were observed for different parameters after Ansys and applying generative design concept for each iteration as follows.

Table 4.15: Observed Values of different Parameters

	Beneficial		**Non-Beneficial**			
Iteration	**Geometry**	**Stiffness**	**Mass (Kg)**	**Stress (MPa)**	**Deformation (mm)**	
1	4	5893.79	11.08	35.582	0.33934	
2	5	2140.87	11.41	25.502	0.9342	
3	2	1057.08	8.75	53.634	1.892	
4	1	1948.18	10.8	23.002	1.0266	
Max	**5**	**5893.79**	**8.75**	**23.002**	**0.33934**	**Min**

For decision-making by using multi-criteria here considering the maximum value of beneficial criteria and minimum value of non-beneficial criteria. After dividing these values to actual values will get the multiplication factor as follows.

Table 4.16: Multiplication Factors for Parameters

	Beneficial		**Non-Beneficial**		
Iteration	**Geometry**	**Stiffness**	**Mass**	**Stress**	**Deformation**
1	0.8	1	0.7897111913	0.6464504525	1
2	1	0.3632416493	0.7668711656	0.9019684731	0.363241276
3	0.4	0.1793548803	1	0.4288697468	0.1793551797
4	0.2	0.3305479157	0.8101851852	1	0.3305474381

After getting multiplication factors will assign the weightage to each criterion as per importance in tadpole structured electric vehicle and get the total weightage for deciding the optimized iteration of swing arm for tadpole EV.

Table 4.17 : Total Weightage of Parameters and Ranking

	Beneficial		**Non-Beneficial**			**Total**	
Weightage	20	25	20	20	15	100	
Iteration	**Geometry**	**Stiffness**	**Mass**	**Stress**	**Total Displacement**	**Total**	**Ranking**
1	16	25	15.79422383	12.92900905	15	84.7232	1
2	20	9.081041232	15.33742331	18.03936946	5.448619139	67.9064	2
3	8	4.483872008	20	8.577394936	2.690327696	43.7515	4
4	4	8.263697892	16.2037037	20	4.958211572	53.4256	3

4.2.3 Rear Wheel Swing arm assembly

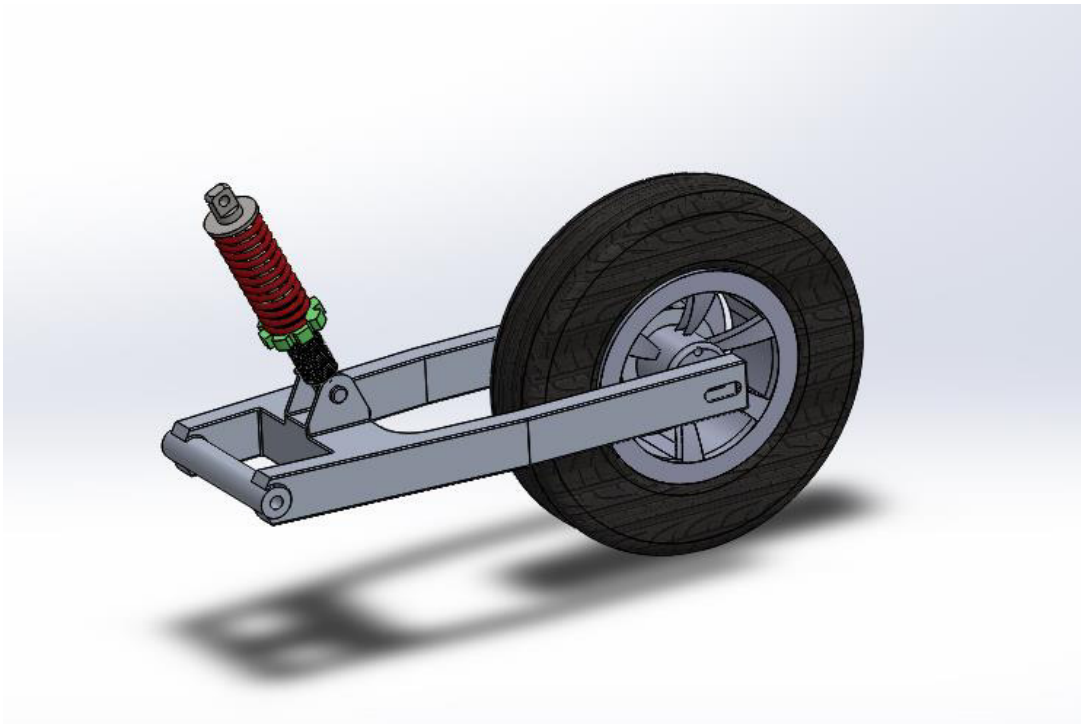

Fig. 30 : Rear wheel Assembly including Mono-shock Suspension

4.3 Design of front wheel assembly and Suspension system

Table 4.18 : Initial Design considerations for Front Wheel Assembly

Parameter	Value
Ground clearance	178 mm
C.G. from ground	400 mm
Wheel base	1800 mm
Track Width	1200 mm
Tire Rate	818154 N/m
Camber	0^o
Castor	0^0
Kingpin Inclination	3^o
Toe Angle	0^0

1. Estimation of maximum weight with driver

Weight on each front Axle/tire

$$W1 = 55 \text{ Kg}$$

$$W2 = 55 \text{ Kg}$$

$$W_f = 110 \text{ Kg}$$

Weight on rear Axle/tire:

$$W3 = W_r = 170 \text{ Kg}$$

Total weight (W) = 280 Kg

2. Design Calculations

Table 4.19: Design Considerations & Parameters

Parameter	Value
C.G. height(z)	406 mm
Roll center height (h)	238 mm
Distance between C.G. and roll center (H): (z-h)	366 mm
Turning radius (R)	2.5 m
Wheel base	1780
Track width	1320

Parameter	Value
Wheel travel	50 mm jounce 50 mm rebound
Roadway bank angle ($\boldsymbol{\alpha}$)	5^0
Velocity (V)	5 m/s

Considered roll rates:

$$K\Phi_{Front} = 7400\frac{Nm}{Rad}$$

$$K\Phi_{Rear} = 10606\frac{Nm}{Rad}$$

Analytical C.G. position:

$b = \frac{(W1 + W2)}{(W) \times L}$ ..... (4.10)

= 0.6461 m

$a = 1 - b$ ..... (4.11)

= 0.926 m

Horizontal lateral acceleration:

$A_\alpha = \frac{V^2}{R\ x\ g}$ ..... (4.12)

= -1.01 $g^{-1}s$

Lateral acceleration in car system:

$A_\gamma = A_\alpha . \mathrm{Cos}(\alpha) - \mathrm{Sin}(\alpha)$ ..... (4.13)

= -1.01 $g^{-1}s$

Effective weight of car due to banking:

$W_e = W\ X\ A_\gamma$ ..... (4.14)

= 317 kg

Effective weight on front and rear wheels:

$W_{ef} = \frac{W_e b}{L}$ ..... (4.15)

= 130.634 Kg

$W_{er} = \frac{W_e a}{L}$ ..... (4.16)

= 186.88 Kg

Roll angle:

$\frac{\Phi}{A_\gamma} = \frac{(-W\,.\,H)}{(K\Phi_{Front}+K\Phi_{Rear})}$ ..... (4.17)

Φ = -1.14^0

Front and Rear lateral load transfer due to lateral acceleration:

$W_{Front} = A_\gamma . \frac{W}{t} \frac{H\,.K\Phi_{Front}}{K\Phi_{Front}+K\Phi_{Rear}} + \frac{b}{L}.Z$ ..... (4.18)

$$W_{Front} = -33.56 \text{ Kg}$$

$$W_{Rear} = -48.08 \text{ Kg}$$

The magnitude of $A_\alpha.\text{Cos}(\alpha)$ is greater than magnitude of $\text{Sin}(\alpha)$ thus, the outside wheel load increases.

Therefore, Front & Rear outside load:

$W_{fo} = \frac{W_{ef}}{2} + 48.08$ ..... (4.19)

= 98.79 Kg

Similarly,

W_{ro} = 141.66 Kg

Change in static load measurement on ground:

$\Delta W_{front} = W_{fo} - W_{Front}$ ..... (4.20)

= 38.79 kg

Similarly,

$$\Delta W_{rear} = \mathbf{55.47\ Kg}$$

Specific ride rate:

$K_{Rf} = \frac{\Delta W_{front}}{Wheel\ Travel}$ ..... (4.21)

= 7489.29 N/m

Similarly,

K_{Rr} **= 10700.2 N/m**

Front and Rear tide frequency:

$W_{frf} = \frac{1}{2\pi}\left(\frac{K_{Rf}}{W_{Front}}\right)^{\frac{1}{2}}$ ..... (4.22)

= 1.25 Hz

Similarly,

W_{frr} = **1.23 Hz**

Therefore, $W_{frf} > W_{frr}$

Wheel Center rate:

$$K_{wfront} = \frac{K_t.K_{Rf}}{K_t - K_{Rf}} \quad \text{..... (4.23)}$$

= 7558.479 N/m

K_{wrear}= 10842 N/m

Spring Rate:

$$K_{wfront} = K_{sf}.(IR)^2 \quad \text{..... (4.24)}$$

Assuming Installation Ratio (IR) for front suspension to be 0.75.

Therefore, front spring rate,

K_{sf} **= 13437.3 N/m**

Similarly,

Assuming Installation Ratio (IR) for rear suspension will be 0.5.

Therefore, rear spring rate,

K_{sf}**= 43368 x 2 N/m**

= 86736 N/m

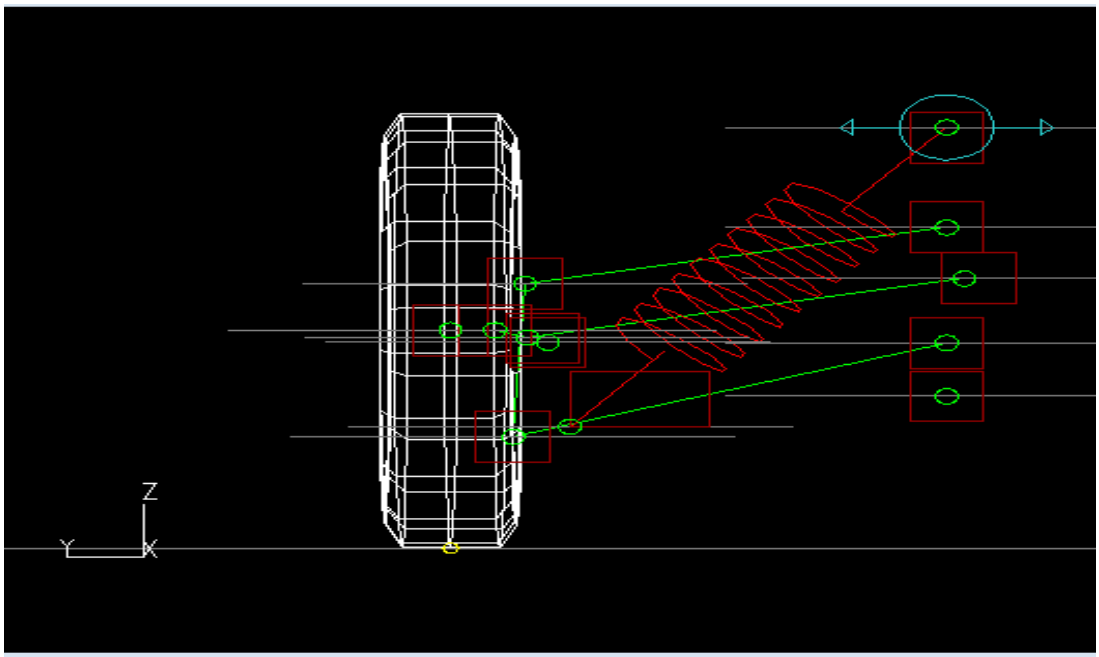

Fig. 31 : Lotus Suspension Analysis

Table 4.20 : Calculated Suspension Parameters

Suspension Parameter	Front	Rear
Type	Double Wishbone	Swing arm
Tire Rate	818.15N/mm	818.15N/mm
Spring Rate	13.4N/mm	86.7N/mm
Installation Ratio	0.75	0.5
Roll angle	1.14^{o}	1.14^{o}
Camber change	1.6875^{o}	0o
Toe angle change	2.16^{0}	00
Castor angle change	0.1870^{o}	00
Kingpin inclination change	0.5319^{0}	00
Halftrack change	1.02 mm	-
Wheelbase change	2.38 mm	-
Un-sprung Mass	20 kg	10 kg

3. Upright

For upright and spindle material selected is **Al 6061 T6** grade because of high tensile strength and light weight characteristics.

Table 4.21: Material Properties of Al 6061 T6

Parameter	Value
Density	2700 Kg/m^3
Youngs Modulus	6.89×10^{10} Pa
Poisson's Ratio	0.33
Yield Strength	2.76×10^{8} Pa
Ultimate Tensile Strength	3.1×10^{8} Pa

A. Load Applied on Upright:

Brake caliper mounting = 1000 N

Steering tie rod joint = 1000 N

Factor of safety: 15

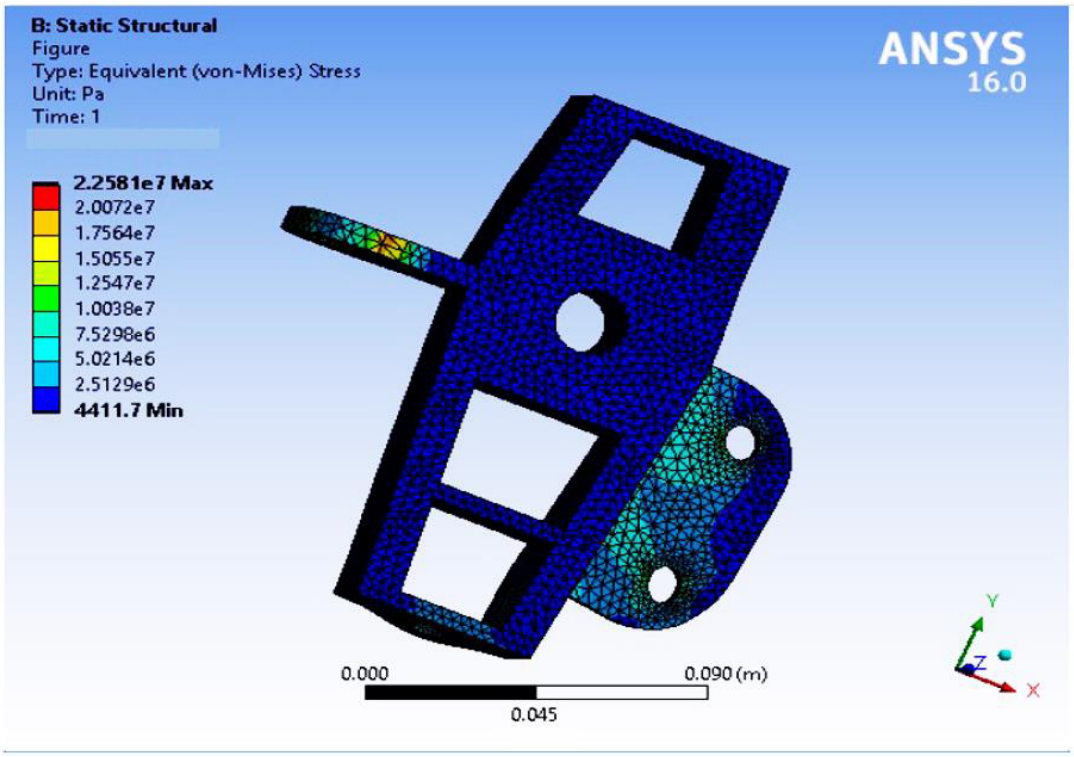

Fig. 32 : Stresses Induced in Upright

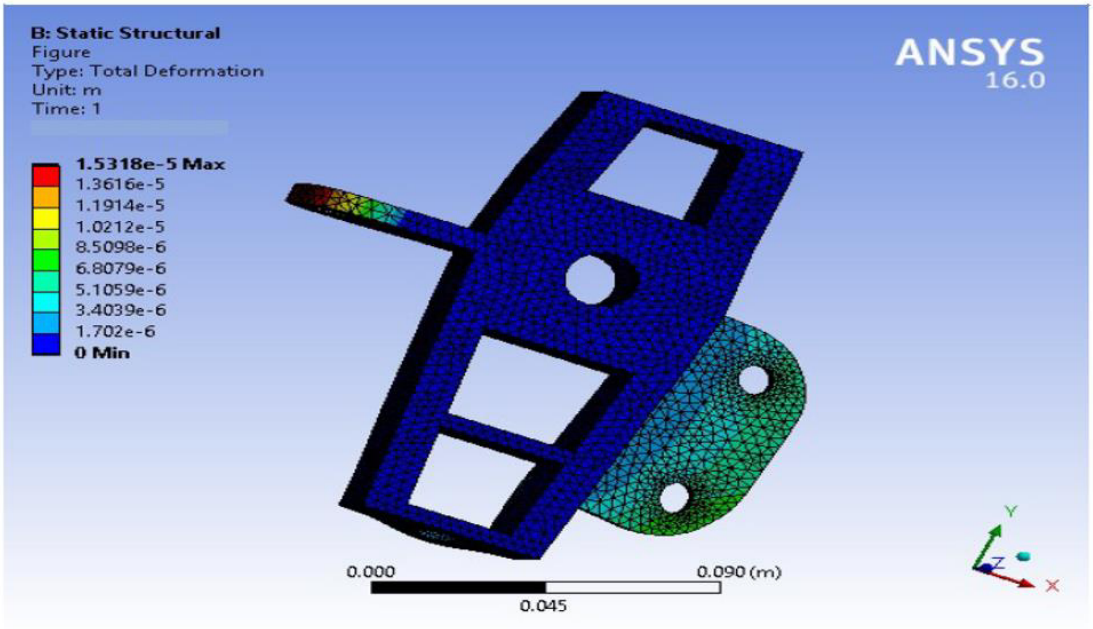

Fig. 33 : Deformation in Upright

1. A-Arms

Material: AISI 4130

Loading condition: 3g

F.O.S: 15

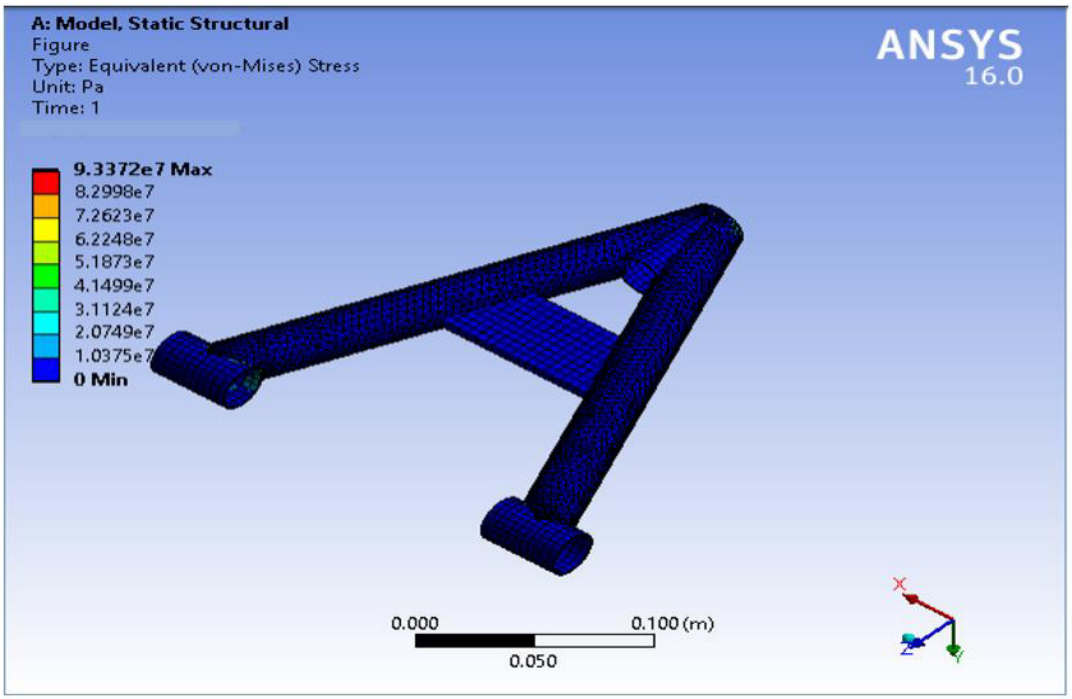

Fig. 34 : Stresses Induced in Lower A- Arm

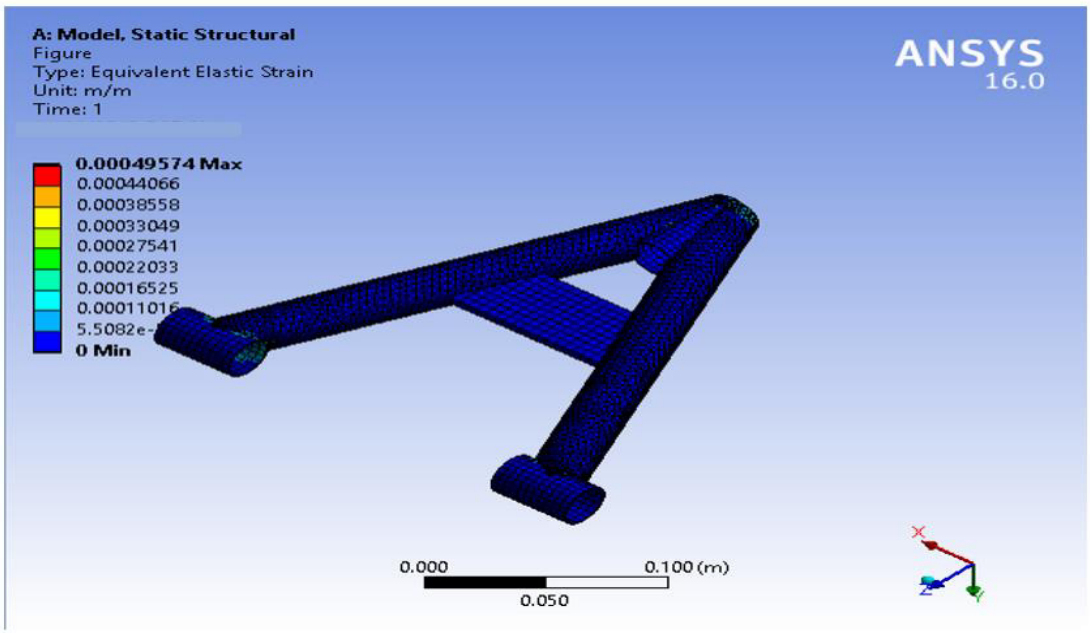

Fig. 35 : Deformation in Lower A- Arm

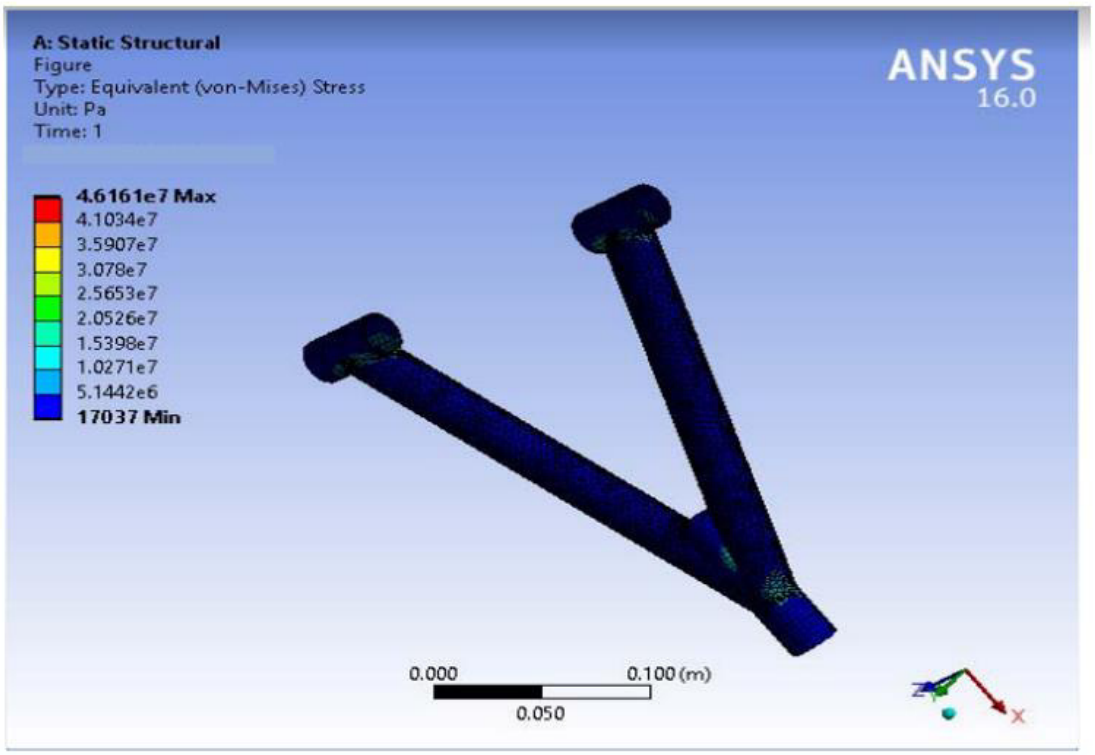

Fig. 36 : Stresses Induced in Upper A- Arm

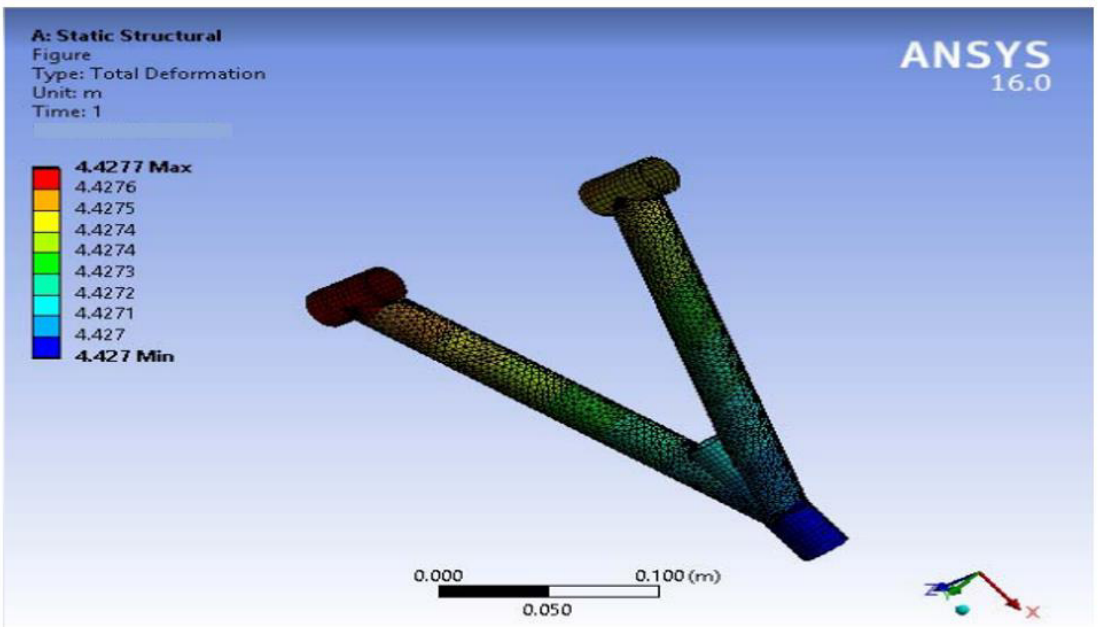

Fig. 37 : Deformation in Upper A- Arm

2. Front Wheel Assembly

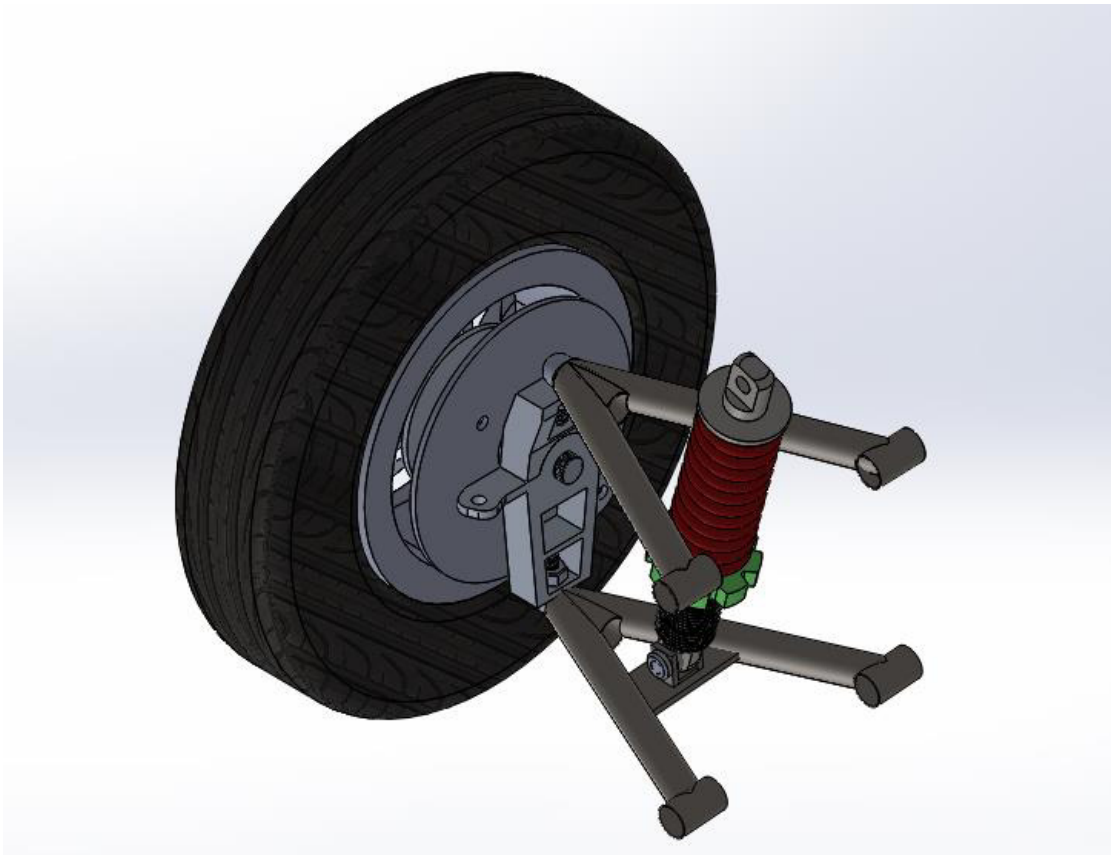

Fig. 38 : Front Wheel Assembly

4.4 Steering System

1. Requirements of steering system:

The steering system must meet the following specifications.

During the maneuvering of the vehicle on a small and curving route, it is imperative for the steering system to possess the capability of executing sharp turns with both ease and fluidity. During a turn, the driver needs to counteract the self-aligning torque by firmly gripping the steering wheel to ensure a seamless recovery of the vehicle. Upon completing the turn, the wheels realign themselves to the straight-ahead position as a result of the self-aligning torque, which occurs when the driver releases the force applied to the steering wheel. The objective is to ensure that there is no loss of steering wheel control and no transfer of kickback caused by road surface roughness and imperfections.

2. Purpose:

The primary function of the steering system is to enable the driver to manipulate the trajectory of the vehicle by rotating the front wheels. The steering wheel serves the purpose of controlling the steering operation. The steering column serves to connect the steering wheel and the pinion. Steering gears are responsible for converting the torque applied to the steering wheel, transmitting it through the steering linkage, and causing the car to turn. A steering linkage refers to the interconnected rods and arms that transfer the motion from the steering gear to the front wheels, enabling them to turn left or right.

3. Ackermann geometry:

- **Turning Radius and Angle:**

$$R=\frac{L}{sin\emptyset}+\frac{T-C}{2} \quad \text{..... (4.24)}$$

$$\text{Sin}Ø = 0.67$$

$$Ø = 42.067^0$$

$$cot\Theta - \text{cot}Ø = \frac{L}{T} \quad \text{..... (4.25)}$$

$$\Theta = 22.24^0$$

$$\text{Total angle} = 64.3^0$$

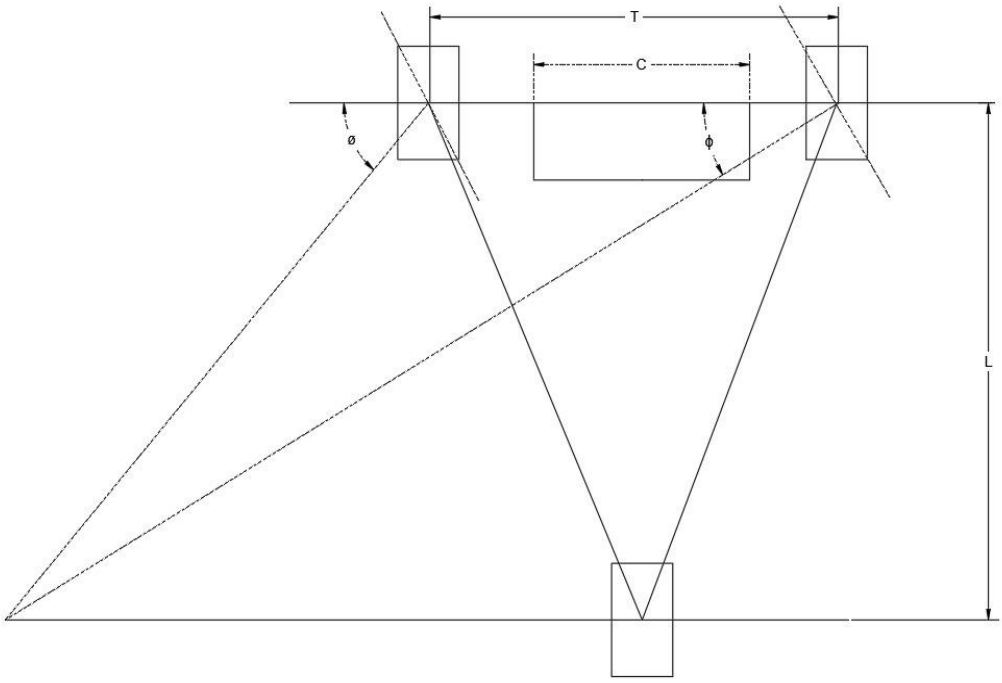

Fig. 39 : Ackermann geometry for Tadpole Structure

Steering ratio = $\frac{360}{64.3}$

= 6:1

Ackerman percentage = 56.31

Turning radius = 3545.86 mm

Kingpin Inclination = 3.03^0

Radius of steering wheel (r) = 127 mm

= 0.127 m

Torque required (T_s) = f × d × r ……(4.26)

= 15×2×0.127

= 3.81N-m

Total rack travel=70 mm turn

=1.5 turn

Hence, rack travel for one rotation of pinion (X_O) = 46.667 mm

$X_0 = 2\pi r$…… (4.26)

r = 7.422mm

Moment ratio = $\frac{Input}{Output}$…….. (4.27)

= $\frac{R}{r}$

Moment ratio = 21.74 : 1

Output load = f × 2 × Moment ratio……. (4.28)

Output load = 652.2N

Table 4.22 : Double wishbone, damper to lower wishbone Incremental Geometry Values

Rack Travel (mm)	Toe Angle RHS (deg)	Toe Angle LHS (deg)	Camber Angle RHS (deg)	Camber Angle LHS (deg)	Ackermann (%)	Turning Circle Radius (mm)
-30.00	-26.03	21.00	0.53	0.23	56.31	3545.86
-25.00	-21.30	17.38	0.39	0.17	63.91	4389.12
-20.00	-16.88	13.76	0.29	0.14	79.98	5622.44
-15.00	-12.68	10.14	0.22	0.11	116.69	7648.59
-10.00	-8.64	6.49	0.16	0.09	223.78	11708.59
-5.00	-4.74	2.81	0.13	0.09	806.64	24726.5

Rack Travel (mm)	Toe Angle RHS (deg)	Toe Angle LHS (deg)	Camber Angle RHS (deg)	Camber Angle LHS (deg)	Ackermann (%)	Turning Circle Radius (mm)
0.00	-0.93	-0.93	0.10	0.10	510.57	94070.7
5.00	2.81	-4.74	0.09	0.13	806.64	24726.5
10.00	6.49	-8.64	0.09	0.16	223.78	11708.59
15.00	10.14	-12.68	0.11	0.22	116.69	7648.59
20.00	13.76	-16.88	0.14	0.29	79.98	5622.44
25.00	17.38	-21.3	0.17	0.39	63.91	4389.12
30.00	21	-26.03	0.23	0.53	56.31	3545.86

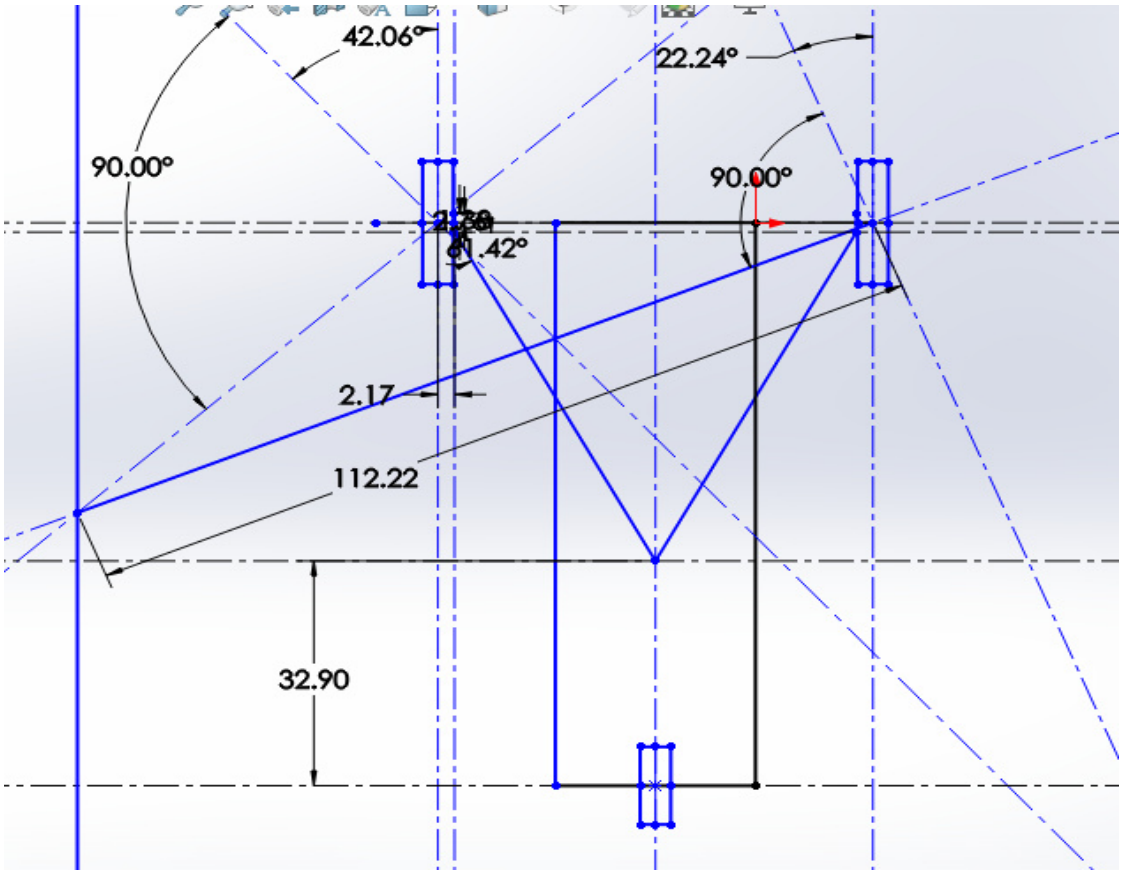

Fig. 40 : Steering Parameters Analysis

4. Result:

Table 4.23: Steering System Parameters

PARAMETERS	VALUE
Wheelbase	1875 mm
Track width	1333.5mm
Inner lock angle	42.06 degree
Outer lock angle	22.24 degree
Camber	0 degree
Castor	0 degree
Kingpin inclination	3.03 degree
Scrub radius	43mm
Toe angle	0 degree
Turning radius	3545.5mm
Rack Travel	140mm end to end
Steering ratio	6:1
Ackermann %	56.31 percentage
Rack Length	11.02 inch

4.5 Battery Selection

1. Battery Type: Lithium-ion battery pack

Chemistry of Cell: $LiFePO_4$.

Chosen the Lithium-ion battery pack due to its lower weight. Research is currently centered around the light weight design strategy. In order to maintain the weight of our car, the lithium-ion battery is a superior choice compared to other existing alternatives. The Battery Management System (BMS) is included with the lithium-ion battery pack. Therefore, it is more secure than a lead-acid battery pack.

Table 4.24 : Selected Battery Pack Specification

Parameter	Value
Nominal Voltage	48 V
Battery Capacity	80 Ah
Low Voltage Cut-Off	41.6 V

Parameter	Value
High- Voltage Cut- Off	57.6 V
Operating Temperature	55^0 C
IP Rating	64
C Rating	0.5 C

2. Selection Criteria:

Availability: The standard voltage sizes are multiples of 12 volts, such as 12V, 24V, 36V, 48V, and 60V.

Cost: As the quantity of cells in the battery pack rises, the total cost of the pack will also increase.

Weight: As capacity increases, the weight of battery pack also increases.

Motor Voltage: Motor, battery and controller voltage should match.

To optimize all above mentioned parameters battery voltage is selected as 48 V and capacity of 80 Ah for development of prototype with minimum cost, minimum weight within the available options of voltage ratings.

3. Power Consumption (P):

P = VOLTAGE * CAPACITY

= 48 * 80

= 3840 Watt.

4. Continuous Run Time of Battery Pack:

Capacity: C = 80 AH

Operating Voltage: V = 48 volt

Average current consumption by motor: I = 25 Amps

Total run time: $T = \frac{C}{I}$

$= \frac{80}{25}$

= 3.2 Hours

Theoretical Range: At Average speed of 50 kmph for 3.2 hours and 20% SOC at the end we can get range of 150 Km.

4.6 Braking System Design

1. Requirements of Braking System

The brakes on the front and rear should be capable of locking the wheels simultaneously. There must be a balance between the amount of clamping force generated and the pedal travel as they are inversely related. The braking torque generated at optimum pedal effort and travel should be much greater than the required braking torque. There should be a provision of two independent hydraulic systems to ensure braking even during failure of one of the systems. [43] The braking torque generated should not be such that the vehicle topples over and loses contact with the ground. In this research, vehicle has incorporated an all-wheel disc braking system is chosen due to its numerous benefits and the simplicity of its installation and maintenance.

The following criteria and parameters were considered during the design of the all-wheel disc brake system:

Table 4.25 : Braking Parameters and Values

PARAMETERS	VALUES
Front Disc diameter	228 mm
Rear Disc diaeter	228 mm
Front Caliper piston diameter	64 mm
Rear Caliper piston diameter	64 mm
Coefficient of friction (μ_r)	0.7
Coefficient of friction (μ_p)	0.6
Master Cylinder Bore Diameter	127 mm
Maximum Velocity	60 Km/h
Maximum Weight of vehicle considered	280 kg

A single pedal, which is aligned with two separate master cylinders, controls the hydraulic braking system. The implementation of two separate master cylinders functions as a safety measure, guaranteeing that in the case of a fault in one cylinder, the other cylinder remains operational. Another advantage of using dual master cylinders is the ability to precisely adjust the braking bias. The braking circuit used is rectangular in shape. This particular approach was used due to the tires' possession of

a positive scrub radius. Therefore, the front braking system will be controlled by one cylinder, while the rear system will be controlled by the other cylinder.

2. Caliper Selection

All three calipers are of the floating type due to their compactness and ease of installation on automobiles. Furthermore, they possess a reduced number of potential areas for leakage in comparison to fixed piston variants.

3. Master Cylinder Selection

Each Master cylinder forms an individual hydraulic braking circuit. Similar master cylinders were chosen for rear and front as a bias bar was installed to distribute pressure proportionately to the front and rear. The brake circuit designed is of horizontal split type. One cylinder will control the front braking and the other the rear system.

4. Pedal

The pedal was designed by keeping in mind that, It should be able bear the load of 2000N. Light weight and feel comfortable to the driver. In case of excessive pedal travel i.e. brake failure due to leakage etc.., a brake over travel switch is to be activated resulting in complete shutdown of the electrical systems. A pedal ratio of 6:1 is selected by considering master cylinder bore size, caliper piston diameter, pedal travel etc. A force of 2000N applied on the pedal pad with the inner circle for balance bar in the pedal as the fixed geometry. Aluminium is the material selected based on its density and yield stress.

5. Braking Calculations

Force/Pressure exerted on MC Bore - F_{mc}/P_{mc}

Force/Pressure developed on calipers – $\frac{F_c}{P_c}$

Clamping force on each wheel – $\frac{F_{CF}}{F_{CR}}$

Effective rotor radius - r_e

Max. Retardation – a

MC Bore area – A_{mc}

Caliper piston area – A_c

Mechanical leverage (m)= 6:1

Force acting on the master cylinder:

$$F_{mc} = m\ x\ F_p \quad \text{..... (4.28)}$$

= 8776.2444 N

Area of master cylinder (piston/bore):

$$A_{mc} = \pi \frac{b^2}{4} \quad \text{..... (4.29)}$$

= 2516 mm^2

Pressure generated:

$$P_c = \frac{F_{mc}}{A_{mc}}$$

= 3.48 N/mm^2

Area of caliper:

$$A_{cp} = \pi \frac{{d_{cp}}^2}{4} \quad \text{..... (4.30)}$$

= 2542 mm^2

Force on caliper:

$$F_{cp} = P_c\ X\ A_{cp} \quad \text{..... (4.31)}$$

= 8776.244 N

By two caliper pistons:

$$F_c = 2F_{cp}$$

= 17552.48 N

Force on disc:

$$F_d = \mu\ x\ F_c$$

= 10531.488 N.

Braking Torque:

$$T_b = F_d\ x\ \frac{D_d}{2} \quad \text{..... (4.32)}$$

= 1069.97 N-m

Braking Force:

$$F_b = \frac{2T_b}{D_w} \text{ .....(4.33)}$$

= 4680.661 N

On two tires = 9361.322 N

Stopping Distance:

Table 4.26 : Braking Parameters

Parameter	Case-I	Case-II
Distance (S)	5 m	2 m
Initial Velocity (u)	40 KMPH	40 KMPH
Acceleration (a)	-12.34 m/s^2	-30.85 m/s^2
Inertia Force (F)	3209 N	8023 N
Energy Generated	15146 J	16046 J

As **F_b > ma,** Therefore, braking is effective.